



Communication

Study on the AE characteristics of fracture process of mortar, concrete and steel-fiber-reinforced concrete beams

Keru Wu*, Bing Chen, Wu Yao

State Key Laboratory of Concrete Materials Research, Tongji University, Siping Road 1239, Shanghai 200092, People's Republic of China

Received 21 April 2000; accepted 29 June 2000

Abstract

The acoustic emission (AE) signals from mortar, concrete and steel fiber reinforced concrete beams during the entire fracture process were recorded and analyzed. Different filters were set on the AE signal duration based on the characteristic of amplitude distribution. From the value of AE signal amplitude, which corresponds to the occurrence of the peak for AE hits, the AE signals from mortar, concrete and steel reinforced concrete were divided into five, seven and nine sections, respectively. The relationship between the AE signal section and the failure mechanism of these materials, analyzed on the meso-structure level was determined. Based on the experiments, the AE characteristics of each failure mechanism are given. The results show that the AE technique is a valuable tool to study the failure mechanism of concrete. © 2000 Elsevier Science Ltd. All rights reserved.

Keywords: Concrete; Mortar; Fiber reinforcement; AE

1. Introduction

The acoustic emission (AE) technique, a tool for non-destructive evaluation of metallic and nonmetallic materials and engineering structure has been used widely. Recently, it has also been applied to studies of concrete mechanics, with a focus on the properties of crack extension during the fracture process [1–4].

AEs are stress waves caused by the sudden release of strain energy resulting from a crack propagating in a material; which contain abundant information on material failure. This information can be applied to detect fracture process and changes of properties in the concrete. Materials fail by different mechanisms, and each mechanism contains certain distinct AE signal parameters. Ely and Hill [5,6] showed that AE signals in graphite–epoxy specimens could be separated into distinct amplitude bands by sorting on the basis of the duration and rise time of the AE signals, which corresponds to matrix cracking, fiber breaking and delaminations. These AE signal parameters can in principle be used to isolate the failure mechanism

by analyzing the amplitude, counts, energy, duration and rise time of the AE.

In this research, the AE signals from steel fiber concrete, normal concrete and mortar during the entire fracture process were recorded, and different filters were set on the AE signal duration according to the characteristic amplitude distributions. The results showed that AE signals, which come from mortar, concrete and steel-fiber concrete, could be divided into five, seven and nine sections, respectively. The relationship between the particular AE signal section and the failure mechanism of these three materials could be analyzed in terms of their meso-structural characteristics.

2. Experiment*2.1. Testing equipment*

The three-point loading flexural tests were performed using an Instron 8501 Digital Servo hydraulic testing system. The specimen dimensions were $100 \times 100 \times 515$ mm, with single edge notch with a depth of 50.0 mm, as shown in Fig. 1. Six PACR15 transducers with a resonant frequency of approximately 150 kHz were mounted on the two opposite surfaces of the specimens to monitor the

* Corresponding author. Tel.: +86-21-6598-2412; fax: +86-21-6598-3465.

E-mail address: wukeru@online.sh.cn (K. Wu).

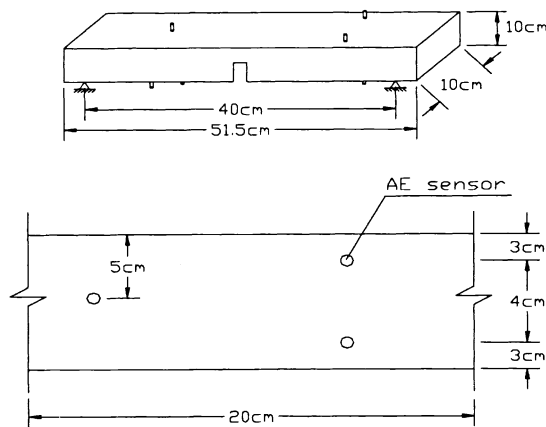


Fig. 1. Geometry of specimen and position of transducers.

AE activities. Midspan deflection of the beam was also measured. The full details of the experiment are given in Ref. [7].

A SPARTAN-AT2000 AE system manufactured by Physical Acoustic was used for AE data acquisition. The AE signals were amplified with a 40-dB gain in a preamplifier and a 20-dB gain in the system. The threshold was set at 40 dB to eliminate a high signal/noise ratio.

2.2. Sample preparation

Three kinds of beams were prepared in this study: mortar, normal concrete and steel-fiber-reinforced concrete, respectively. The specimens were demolded 1 day after casting, and then were cured in a fog room at 17–23°C and greater than 90% relative humidity. Two days before test at 28 days, they were taken out for the cutting of a single edge notch. The mix proportions are shown in Table 1.

3. The principle of isolating failure mechanisms

3.1. Basic principle

The deformation and rupture of materials are often attributed to different mechanisms, each of which emit certain AE signals. The AE signals that the transducers receive during the entire failure process contain information on all of the various failure mechanisms of concrete, which overlap. In order to isolate the AE signal associated with each of the different failure mechanisms, a method

was proposed according to the following hypotheses: (1) For the same AE activity, the higher the energy it emits, the higher the amplitude and the longer its duration; (2) AE activities associated with the same failure mechanism have the same characteristics. To isolate the different AE characteristics produced by the different mechanisms, different filters were set on the AE duration. When a certain duration was selected, three graphs were plotted: (a) plot of hits versus amplitude; (b) plot of counts versus amplitude; (c) plot of hits versus counts. At the same time, the shapes and the characteristics of the three graphs were compared. If the peak of the hits versus amplitude graph in (a) is the same as that of the counts versus amplitude graph in (b), while the counts/hits ratio calculated from the data of (a) and (b) is referred to the peak of the hits versus counts graph in (c), then we can say there is only one failure mechanism contained for this time duration. Based on the above principle, different failure mechanisms occurring during the deformation and rupture of concrete can be separated.

3.2. Example

During the fracture of an SFRC beam under three-point loading test, a total of 199,275 hits and 1,771,822 counts were recorded. Fig. 2 shows the data plotted as: (a) hits versus amplitude, (b) counts versus amplitude and (c) hits versus duration. In Fig. 2a, the peak of 11,000 hits occurred at 40 dB, followed by an approximately exponential decay in the number of hits with increasing amplitude. Fig. 2b shows the peak of the counts versus amplitude plot at 55 dB, which drops 5 dB behind the 40-dB peak seen in Fig. 2a.

From Fig. 2a and b, it was found that the peaks of hits versus amplitude, and count versus amplitude plots are different, which indicates that different failure mechanisms overlap. Therefore, the AE signal was isolated based on the hypothesis discussed above, with different filters set for duration.

3.2.1. The first step

The first step was to isolate the failure mechanism corresponding to the lower amplitude. Therefore, the first filter was set with a 0–25 μ s duration interval. Since low amplitude signals had a characteristically shorter duration than the larger amplitude signals, to ensure that all of hits corresponding to the lower amplitude were included, a second and a third filter were set with 0–30 μ s and 0–35 μ s duration, respectively. As

Table 1
Details of concrete mix proportions

Series	Water (kg/m ³)	Cement (kg/m ³)	Slag (kg/m ³)	Sand (kg/m ³)	Gravel (kg/m ³)	Steel fiber (kg/m ³)
Mortar	176	518	202	1032		
Normal concrete	176	472	202	632	948	
Steel-fiber concrete	176	472	202	632	948	70

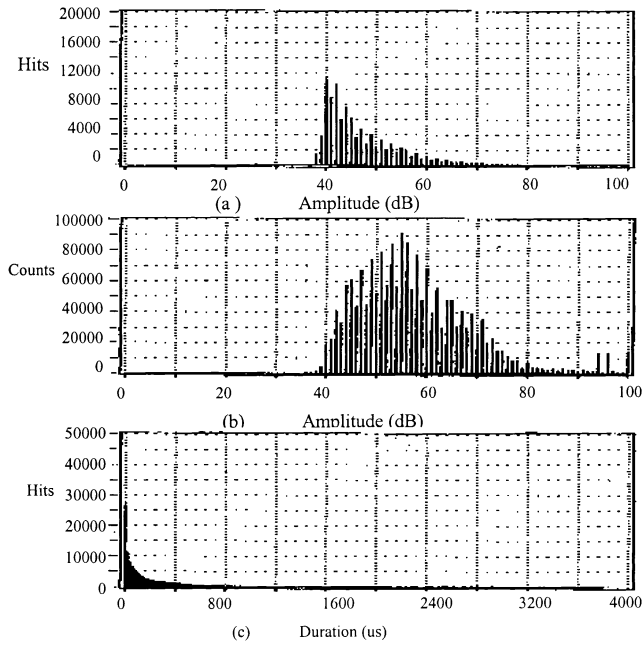


Fig. 2. Original data of steel-fiber concrete.

the results shown, a duration interval from 0 to 35 μs was found to be appropriate for isolating the failure mechanism corresponding to the lower amplitude. The hits versus amplitude plot shown in Fig. 3a displays a single distribution with a peak amplitude at 40 dB, with a total of 35,066 hits and 65,620 counts, resulting in a counts/hits ratio of approximately 1.87. The counts versus amplitude plot shown in Fig. 3b also has its peak at 40 dB with a single distribution such as

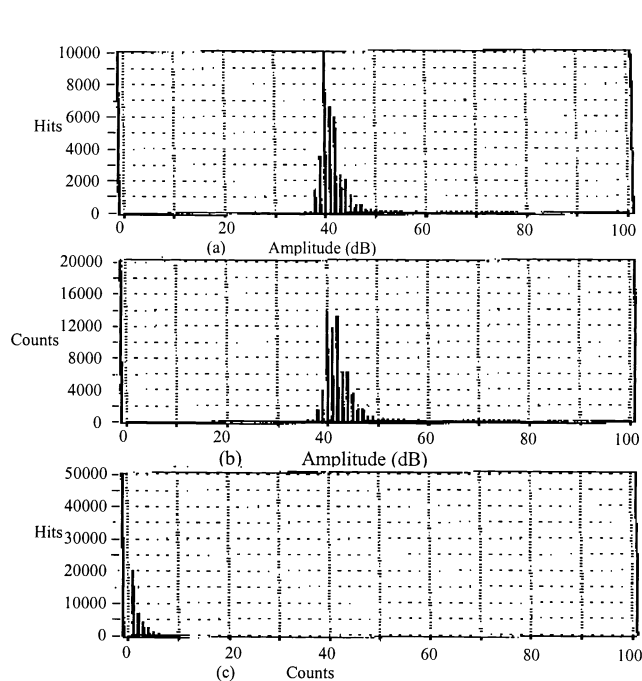


Fig. 3. AE signal of mechanism 1.

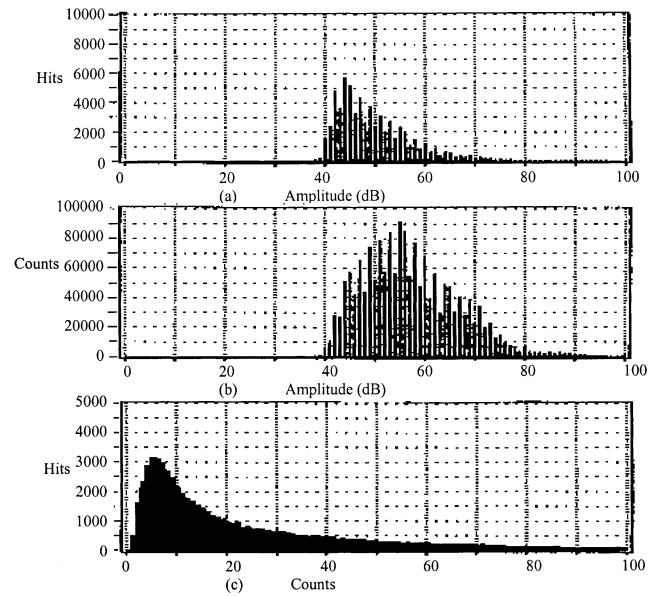


Fig. 4. Original data without mechanism 1.

that of Fig. 3a. Fig. 3c shows that the hits versus counts plot has its center at a value of approximately 1.87, the same as the counts/hits ratio calculated from the data of Fig. 3a. This confirms that there is only a single predominant failure mechanism presented in Fig. 3, which is labeled as mechanism 1. The distribution of amplitude starts at about 36 dB and ends at 50 dB. The hits having amplitudes greater than 50 dB can be disregarded since they probably represent overlap from other mechanisms.

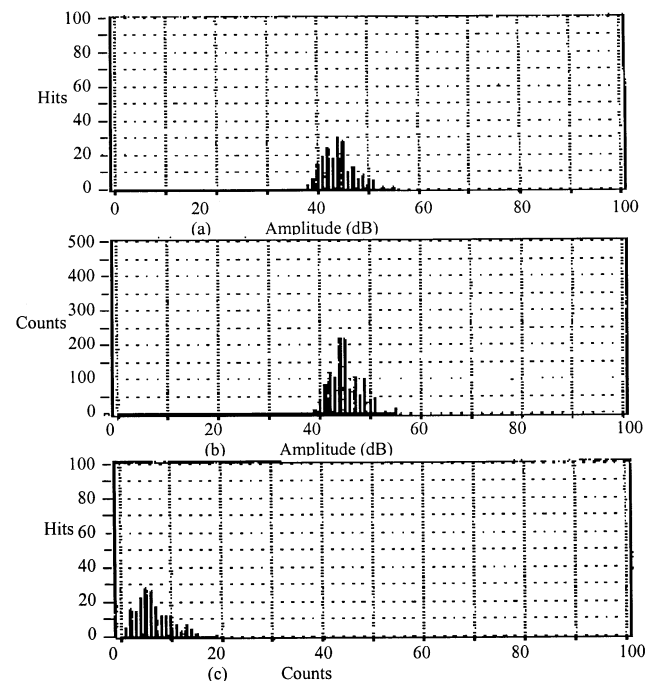


Fig. 5. AE signal of mechanism 2.

3.2.2. The second step

Having isolated mechanism 1, it was then removed from the original data by filtering on a duration greater than 35 dB. The results obtained using this filter for the hits versus amplitude plot on amplitude distribution is shown in Fig. 4a. This figure represents the original data without mechanism 1. It has a peak at 44 dB and includes 64,209 hits and 1,706,202 counts, resulting in a ratio of 26.5 counts/hits. Fig. 4b shows peak of counts versus amplitude plot at 56 dB, which is different from the 44 dB peak seen in Fig. 4a. As a result, the shapes are also slightly different. This indicates that there are signals present from sources with different counts/hits ratios. The peak in Fig. 4c is located at 5 counts, which is different from the 26.5 calculated from the data of Fig. 4a; thus, there are at least two overlapping distributions (failure mechanisms) present, which need to be analyzed further.

Following the first step, the remain AE signals can be divided into eight sections and labeled as mechanisms 2, 3, 4, 5, 6, 7, 8 and 9. Fig. 5 is the graph of mechanism 2.

4. Results and discussion

Figs. 6 and 7 show the original AE signals of normal concrete and mortar, respectively. According to the method presented above, the AE signals from normal concrete and mortar were divided into seven and five

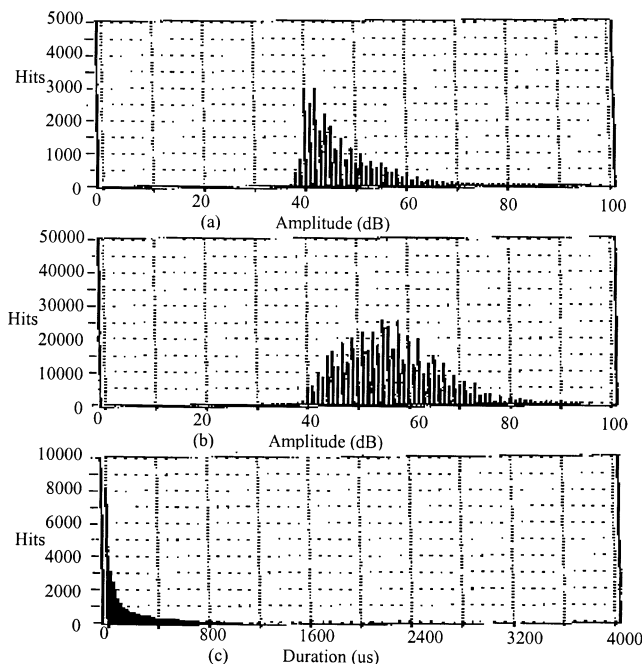


Fig. 6. Original data of normal concrete.

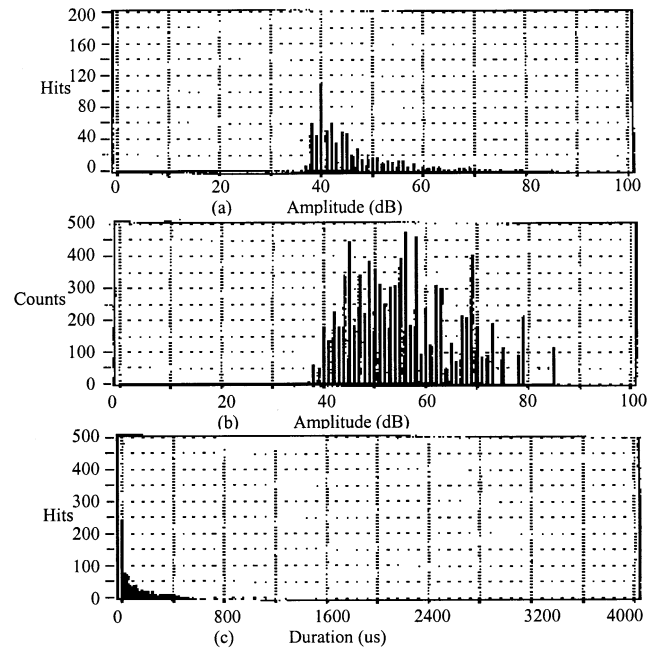


Fig. 7. Original data of mortar.

sections, respectively. Tables 2, 3 and 4 present a summary of the AE parameter characteristics for different failure mechanisms.

From the results above, the number of failure mechanisms of mortar was two less than that of normal concrete. Among these failure mechanisms, the AE parameter characteristics of mechanisms 1 to 7 for concrete are the same as mechanisms 1 to 7 for steel-fiber-reinforced concrete. From the experiments, mechanisms 8 and 9 both occurred at or near beam failure and emitted high-energy signals. They can be thus considered as steel fiber pullout and breaking, respectively. The duration of mechanism 2 for mortar is nearly equal to the sum of the duration of mechanisms 2 and 3 for normal concrete and steel-fiber concrete, while the position of the peak of the hits and the amplitude distribution are similar to mechanism 3 for normal concrete and steel-fiber concrete. As we know, there is only fine aggregate in mortar, while normal concrete and steel-fiber-reinforced concrete contain both fine and coarse aggregates. According to the distribution of amplitude and the percent of total hits (steel fiber concrete 18.5%, normal concrete 17.0%), mechanism 2 for mortar and mechanism 3 for concrete and steel-fiber-reinforced concrete are believed to be the development of bond cracks between the cement paste and the fine and coarse aggregates, respectively. Mechanism 7 is apparently related to crack extension through the coarse aggregate, which emits high-energy signals. Mechanism 1, 4, 5 and 6, may be related to cracks initiating and progressing in cement paste, which include micro flaws aggregation,

Table 2
AE parameter characteristics for the steel-fiber concrete failure mechanisms

Mechanism	Amplitude distribution			Duration (μ s)	Hits	% of total hits	Counts
	Peak (dB)	Range (dB)	Counts/hits				
1	40	36–54	1.87	0–35	35066	35.3	65620
2	42	38–59	4.73	35–60	10588	10.67	50138
3	44	40–60	9.0	60–130	18319	18.5	164756
4	47	42–64	16.7	130–220	12024	12.1	212829
5	51	43–66	31.7	220–355	10274	10.35	326176
6	56	47–70	53.2	355–555	7665	7.72	408902
7	62	51–75	82.6	555–800	3335	3.35	275786
8	71	55–83	114	800–1080	1305	1.31	149043
9	73	62–100	149.6	1080–4000	699	0.7	118572

Table 3
AE parameter characteristics for normal concrete failure mechanisms

Mechanism	Amplitude distribution			Duration (μ s)	Hits	% of total hits	Counts
	Peak (dB)	Range (dB)	Counts/hits				
1	40	36–54	1.52	0–25	9248	33.2	14077
2	42	38–59	4.48	25–60	5271	18.9	23648
3	44	40–60	98.7	60–125	4733	17.0	41236
4	47	42–64	17.4	125–220	3287	11.8	57214
5	51	43–66	31.7	220–355	2789	10.0	88999
6	58	47–70	55.8	355–555	1970	7.0	110017
7	62	52–80	104.6	555–800	1433	5.14	150127

Table 4
AE parameter characteristics for mortar failure mechanisms

Mechanism	Amplitude distribution			Duration (μ s)	Hits	% of total hits	Counts
	Peak (dB)	Range (dB)	Counts/hits				
1	40	36–47	1.64	0–35	304	43.3	500
2	44	39–55	6.4	35–125	189	27.0	1218
3	45	42–64	6.9	125–220	99	14.1	1681
4	55	46–64	31.4	220–355	57	8.1	1794
5	58	53–70	64.1	355–555	60	8.0	3847

Table 5
AE parameter characteristics for nine failure mechanisms

	Mechanism								
	1	2	3	4	5	6	7	8	9
Duration (μ s)	0–35	35–60	60–130	130–220	220–355	355–555	555–800	800–1080	1080–4000
Amplitude distribution (dB)	36–54	38–59	40–60	42–64	43–66	47–70	51–75	55–83	62–100
Peak (dB)	40	42	44	47	51	56	62	71	73

micro-crack formation, crack extension, coalescence of the micro cracks and initiation of macro cracks. Table 5 gives the parameter characteristics.

5. Conclusions

1. AE is an effective method for studying the failure mechanism of concrete.

2. AE duration is the primary filter parameter. Different filters were set on the AE duration and the graphs of counts

versus amplitude and hits versus counts were plotted to verify that a single failure mechanism was present in the separated amplitude distribution, and the different failure mechanism can be isolated, respectively.

3. Experimental results indicate that there exist five, seven, and nine distinct failure mechanisms for mortar, concrete and steel-fiber-reinforced concrete, respectively, during the entire fracture process.

4. Based on the experiments, the AE signal parameters for different failure mechanisms involved in steel-fiber-reinforced concrete, concrete and mortar were obtained.

References

- [1] H. Mihashi, N. Nomura, S. Niiseki, Influence of aggregate size on fracture process zone of concrete detected with three dimensional acoustic emission technique, *Cem Concr Res* 21 (5) (1991) 737–744.
- [2] H.L. Chen, C.T. Cheng, S.E. Chen, Determination of fracture parameters of mortar and concrete beams by using acoustic emission, *Mater Eval* 50 (7) (1992) 888–894.
- [3] C.S. Quyang, E. Landis, S.P. Shah, Damage assessment in concrete using quantitative acoustic emission, *J Eng Mech Div Am Soc Civ Eng* 117 (11) (1991) 2681–2698.
- [4] M. Ohtsu, M. Shigeishi, H. Iwase, W. Koyanagi, Determination of crack location, type and orientation in concrete structures by acoustic emission, *Mag Concr Res* 43 (155) (1991) 127–134.
- [5] T.M. Ely, E.v.K. Hill, Characterization of failure mechanisms in graphite/epoxy tensile test specimen using AE data, *Proceedings of Fourth International Symposium on AE from Composite Materials*, Seattle, WA, ASNT, 1992, pp. 187–199.
- [6] T.M. Ely, E.v.K. Hill, Longitudinal splitting and fiber breakage characterization in graphite epoxy using AE data, *Mater Eval* 53 (2) (1995) 288–294.
- [7] D. Zhang, K. Wu, Fracture process zone of notched three-point-bending concrete beams, *Cem Concr Res* 29 (1999) 1887–1892.